"Black box" calibration methods investigated with a virtual fringe projection system

Thomas Böttner*, Dr. Jörg Seewig

Institut für Mess- und Regelungstechnik, Universität Hannover, Nienburgerstr. 17, 30167 Hannover, Germany

ABSTRACT

The mathematical fundamentals of some black box calibration procedures for fringe projection system are introduced. These calibration procedures are based upon a direct mathematical transformation between the measuring volume and the image data obtained with a camera. Aided by a mathematical model of a fringe projection system various calibration procedures are compared to each other in numerical simulations. The numerical simulations facilitate statements about the attainable measuring error depending on the calibration procedure and system parameters.

Keywords: virtual fringe projection system, direct calibration, black box models, 3-D measurement, simulation

1. INTRODUCTION

Fringe projection systems provide a fast and contact-free facility for measuring free-form surfaces in three dimensions. For accurate 3-D coordinate measurements the calibration of the entire fringe projection system is essential. The calibration has to establish the relationship between the 3-D coordinates in the measuring volume and the 2-D coordinates of the camera array associated with the projected fringes. Therefore, the used calibration algorithm directly determines the achievable measuring uncertainty. On the other hand, every calibration algorithm also depends on several measuring parameters, such as the triangulation angle or the measuring volume, for instance. So far, no systematic study has been carried out comparing the different calibration methods. The emphasis of this paper is put on direct calibration methods, also called "black box" methods, which are usually based on polynomial functions. The theoretical advantage of such methods is that they implicitly take into account all error sources, such as lens distortions, for example.

In contrast to that, a physical model[1] of the fringe projection system has to be drawn up for geometrical/physical calibration procedures. The calibration of the fringe projection system is used to determine the unknown parameters of the model that have a physical meaning, such as the inner and outer orientation of both the camera and the projector.

Usually, a fringe projection system consists of a projector as active unit and one or more cameras. In the following, we will talk about systems with only one camera. The projector casts time-wise coded fringe patterns (e.g. Gray-code and phase shift[2]) into the measuring volume while the camera observes the measuring volume.

The fringe projection system gathers all information about the surfaces of the measuring objects with the camera. Thus, all error sources of the fringe projection system ultimately accumulate in the pixels of the camera image. The information from the camera image plus predetermined control points inside the measuring volume are the input parameters of the "black box" calibration algorithms.

For the first time a virtual fringe projection system was implemented on a computer. With this virtual fringe projection system the calibration procedures can be evaluated with respect to their attainable measuring error regardless of the input parameters with failures of a real fringe projection system. Based upon this model, the flaws of every calibration method can be investigated by the means of numerical simulations under ideal conditions, i.e. error-free. Moreover, the impact of any single error source or the variation of a measuring

* E-mail: thomas.boettner@imr.uni-hannover.de; phone +49(511) 762-4278; www.imr.uni-hannover.de

Optical Metrology in Production Engineering, edited by Wolfgang Osten, Mitsuo Takeda, Proc. of SPIE Vol. 5457 (SPIE, Bellingham, WA, 2004) · 0277-786X/04/$15 · doi: 10.1117/12.554748

parameter on the measuring uncertainty can be estimated by the variation of the model parameters of the virtual fringe projection system.

Some "black box" calibration methods (BBCM) are introduced in the following chapter. Afterwards the numerical simulation of the virtual fringe projection system is addressed.

2. "BLACK BOX" CALIBRATION METHODS

At first, some helpful definitions are established. Note that here all vectors are column vectors.

The size of the measuring volume is given by the optical characteristics of both the camera and the projector. It is not clearly demarcated (e.g. due to the depth of sharpness). In a mathematical sense the measuring volume M is a subset of the 3-D space, i.e. $M \subset \mathbb{R}^3$. A point inside the measuring volume is referred to as $(x, y, z) \in M$. Furthermore, an object coordinate system with coordinates X, Y and Z is introduced, with its origin in the center of the measuring volume and the Z direction parallel to the optical axis of the projector. $\mathbf{x}^{\mathrm{T}} = (x, y, z)$ is a point of the latter coordinate system as well.

A sequence of coded light generated by the projector is cast on a measuring object that is brought into the measuring volume. Information about the geometrical dimensions of the measuring object is obtained from the light of the fringe sequence that is reflected from the surface of the measuring object. The amount of light that is reflected from the surface in the direction of the camera provides an relationship between the place of reflection in the measuring volume and the corresponding camera pixel (i, j) due to the time-wise coding of the fringe sequence. All in all, the camera provides a triple $(i, j, \phi) \in B \subset \mathbb{R}^3$ for the point of reflection $p \in M$, where ϕ is the phase based upon the time-wise coding *.

The relation between points $p \in M$ and corresponding camera triples $b \in B$ must be known for taking measurements. The mapping between M and B is accomplished by a calibration function f. The unknown parameters of f, which are also referred to as calibration parameters, are determined by the calibration procedure.

In the case of BBCM the calibration function f is a merely mathematical mapping, i.e. the function directly approximates the relation between the camera triples b and the object points p. In general, the approximation function is a polynomial. The calibration parameters are the corresponding coefficients of the polynomial. During the calibration procedure points with known coordinates inside the measuring volume M must be provided. This can be done with a calibrating device that provides control points with superior accuracy, i.e. the deviations are less than the resolution of the fringe projection system. Often a calibrating plane with plane spread markers and known marker distances is used.

The plane provides only 2-D information. However, information about the entire 3-D measuring volume must be furnished to the "black box" procedure by shifting the calibrating plane. So it is stepped through the measuring volume in the direction of the normal vector of the calibrating plane (usually along the optical axis of the projector). The positions and phase values of the markers in the camera images must be calculated by means of image processing algorithms for every step of the calibrating plane. For extended markers the position can be determined with subpixel methods, i.e. the resolution is better than the camera pixel resolution.

Stepping the calibrating plane through the measuring volume generates a 3-D grid of markers. The number of markers on the calibrating plane and the increment of each step determine the density of the 3-D grid inside the measuring volume.

2.1. Mathematical description

All calibration procedures that are introduced here are based upon polynomials as a mapping between points of the set M (measuring volume) and points of B where the order of the polynomial should always be N for simplification. Furthermore, the following definitions apply.

*Actually the image pixel are natural numbers but with subpixel methods they can also be real numbers.

Coefficient vectors contain the coefficients of the polynomial. They are denoted as symbols from the beginning of the alphabet:

$$\begin{aligned} \mathbf{a}^{\mathrm{T}} &= (a_{000}, a_{100}, a_{010}, a_{001}, a_{200}, a_{110}, \ldots, a_{00N}) \\ \mathbf{b}^{\mathrm{T}} &= (b_0, b_1, b_2, \ldots, b_N) \end{aligned}$$

Contrary, vectors containing variables or coordinates - they are referred to as variables vectors - are denoted as symbols from the end of the alphabet:

$$\begin{aligned} \mathbf{u}^{\mathrm{T}} &= (1, X, Y, Z, X^2, XY, \ldots, Z^N) \\ \mathbf{v}^{\mathrm{T}} &= (1, i, j, \phi, i^2, ij, \ldots, \phi^N) \\ \mathbf{w}^{\mathrm{T}} &= (1, i, j, Z, i^2, ij, \ldots, Z^N) \\ \mathbf{p}^{\mathrm{T}} &= (1, \phi_{ij}, \phi_{ij}^2, \ldots \phi_{ij}^N) \end{aligned}$$

So the various BBCM can be formulated as follows.

- Method *A*

  For every coordinate X, Y, Z of the object coordinate system a separate polynomial that is a function of (i, j, ϕ) is used. It is exemplified for the coordinate X. The remaining coordinates are processed likewise.

$$X = f_{X,A}(i, j, \phi) = \sum_{\substack{\nu=0 \\ \nu=\alpha+\beta+\gamma}}^{N} a_{\alpha\beta\gamma}\, i^{\alpha} j^{\beta} \phi^{\gamma} = \mathbf{v}^{\mathrm{T}} \cdot \mathbf{a}, \qquad \nu, \alpha, \beta, \gamma \in \mathbb{N} \tag{1}$$

  This procedure is put to use in Ref. 3, for example.

- Method *B*

  In this case, the Z coordinate is calculated in a different way. For every image point (i, j) of the camera a separate polynomial in the direction of Z is used. This polynomial is only a function of the phase values ϕ_{ij} of the image points that are obtained with every step of the calibrating plane through the measuring volume. Consequently, the phase values ϕ_{ij} of each camera pixel (i, j) for each step of the calibrating plane have to be gathered! Thus, for every camera pixel (i, j) a polynomial of a variable ϕ_{ij} is obtained:

$$Z_{ij} = f_{ij}(\phi_{ij}) = \sum_{\nu=0}^{N} b_{\nu}\, \phi_{ij}^{\nu} = \mathbf{p}^{\mathrm{T}} \cdot \mathbf{b}, \qquad \nu \in \mathbb{N} \tag{2}$$

  The polynomials approximating the coordinates X and Y are the same as in method *A*. Though the polynomials are not a function of ϕ but of the coordinate Z in order to enhance the numerical stability of this method. Consequently, for X, for instance, applies:

$$X = f_{X,B}(i, j, Z) = \mathbf{w}^{\mathrm{T}} \cdot \mathbf{a} \tag{3}$$

- Method *C*

  Here, for i, j and ϕ each time a polynomial is used which is a function of the coordinates X, Y and Z.[5] Thus, the polynomial for i, for instance, reads:

$$i = f_i(X, Y, Z) = \sum_{\substack{\nu=0 \\ \nu=\alpha+\beta+\gamma}}^{N} a_{\alpha\beta\gamma}\, X^{\alpha} Y^{\beta} Z^{\gamma} = \mathbf{u}^{\mathrm{T}} \cdot \mathbf{a}, \qquad \nu, \alpha, \beta, \gamma \in \mathbb{N} \tag{4}$$

In summary, all three methods lead to equations similar to

$$q = \mathbf{t}^{\mathrm{T}} \cdot \mathbf{d} \tag{5}$$

where $\mathbf{d}$ is a coefficient vector, $\mathbf{t}$ is a variables vector and q is a scalar.

The goal of the calibration procedure is to determine the vector $\mathbf{d}$, i.e. the coefficients of the polynomial. This is accomplished by solving an over-determined linear system of equations. Therefore, it is necessary to gather enough triple $b \in B$ with the camera. In this case, every variables vector $\mathbf{t}_k$, where $k = 1 \ldots m$, $m \in \mathbb{N}$, has k corresponding values q_k. Additional premises should be $m \gg \dim \mathbf{d} =: d$ and using the L_2 norm. The result is the linear least squares problem

$$\|\mathbf{q} - \mathbf{A}\mathbf{d}\|_2 \stackrel{!}{=} min \tag{6}$$

where $\mathbf{A}$ is the (Vandermonde) matrix and $\mathbf{q}$ is the vector:

$$\mathbf{A} = \begin{pmatrix} t_1^T \\ t_2^T \\ \vdots \\ t_k^T \end{pmatrix} \in \mathbb{R}^{k \times d} \qquad \text{and} \qquad \mathbf{q} = \begin{pmatrix} q_1 \\ q_2 \\ \vdots \\ q_k \end{pmatrix} \in \mathbb{R}^k$$

Equation (6) can by solved employing a QR decomposition. The result is the coefficient vector $\mathbf{d}$ that also determines the corresponding calibration function.

2.2. Calibration of measurements

Having taken a measurement, the corresponding 3-D object points $(x, y, z) \in M$ have to be calculated from the measured triples $(i, j, \phi) \in B$ of the camera. For this reason, the object points have to be calculated by means of the calibration function f. Methods A and B directly provide the object points via equations (1) or respectively (2) and (3) from the camera triple (i, j, ϕ).

On the other hand, method C leads to a non-linear problem, because the object coordinates are contained only implicitly in equation (4). For solving the non-linear problem, an initial estimate $\mathbf{x}_0^{\mathrm{T}} = (x_0, y_0, z_0)$ must be furnished for every measured camera triple $b_k = (i_k, j_k, \phi_k)$.

Apparently, one can easily process measurements according to methods A and B, because only linear functions are used for both calibration and measuring. However, a compensation of stochastic errors (e.g. the noise of the camera) is only possible with method C (the least square fit is based upon the camera triples with errors). But the calibration according to methods A and B can be subjected to a considerable amount of measuring errors (the least square fit is based upon the object coordinates that are almost ideal anyway).

On the other hand, one does not have to solve a non-linear system of equations.

3. NUMERICAL SIMULATION

In order to evaluate the attainable measuring error of the various BBCM a numerical simulation of a fringe projection system was programmed in Matlab. The simulation provides information about the influence of a variety of parameters on the virtual fringe projection system.

The simulation is based upon a model of a projector and a camera under ideal conditions. In both cases the optical axis is at right angles with the camera plane and the projecting plane of the projector. The optical axes intersect at the center of the measuring volume which is also the origin of the object coordinate system, Fig. 1. The rows of the camera plane parallel the plane of the optical axes. The same applies for the projector plane. A central projection is used for the camera and the projector. The camera brakes down into discrete pixels while the projector provides a continuous fringe pattern in the direction that parallels the plane of the optical axes. The number of fringes on the projector plane is constant in vertical direction.

Starting with this ideal setup, single conditions can be altered, such as the quantization of the determination of the marker positions on the camera plane according to the subpixel methods of a real fringe projection system. Other possibilities are adding noise of a defined parameterization to some components or using optical distortions.

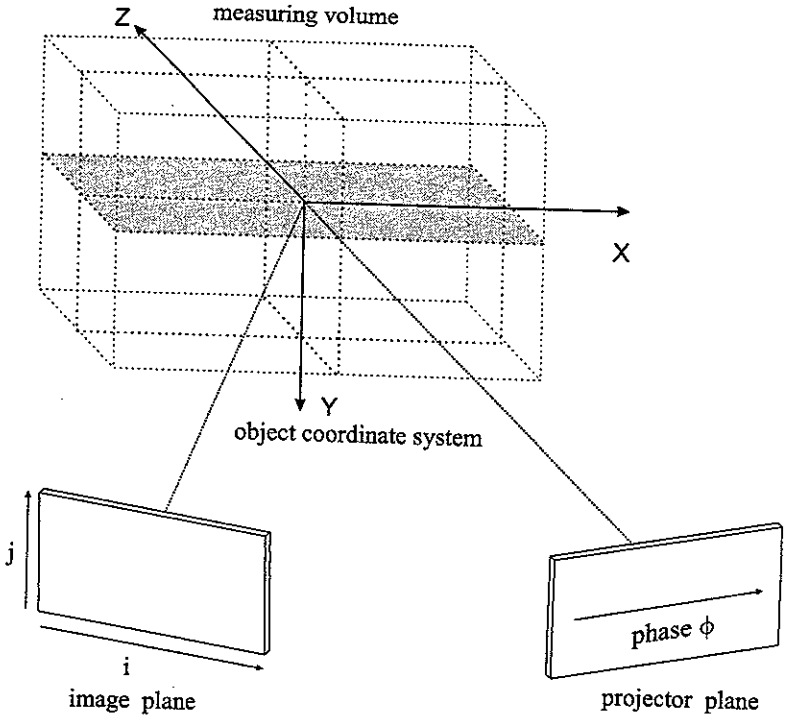

Figure 1. Setup of the virtual fringe projection system

The input parameters used to calculate the calibration parameters are determined in the same way as for a real fringe projection system. Separate object points (markers) or planes (for method B) are brought into the measuring volume at a defined position. For every camera pixel of the camera plane the position and the phase values are obtained. The camera points that correspond to the markers are determined by a direct projection of the markers on the camera plane (regardless of the resolution of the camera). The relevant phase values are determined by a direct projection of the markers on the projector plane.

In order to determine the measuring error, separate spheres are brought into the virtual measuring volume. Based on a central projection and starting from the focus point of the camera in the direction of the measuring volume the intersecting point with the sphere is calculated for every camera pixel. Afterwards, the related phase at the intersecting points (the part of the sphere that is hidden from the projector is omitted) is determined as described above. Here the principle of tracing a ray back to its origin, i.e. a raytracing algorithm, is applied. The same principle is applied for phase values on a calibrating plane as for calibration method B.

The result is a set of points in M with corresponding triples $b_i \in B$, $i = 1 \ldots p$, $p \in \mathbb{N}$. A calibration of this set of points (i.e. of the measurements) based upon the values b_i and the previously calculated calibration parameters provides the 3-D object points $o_i \in M$. From the object points o_i a least square fit for a sphere is done that provides the center and the radius of the sphere. From there statements about the calibration deviation can be concluded.

3.1. Numerical calculations

In this section some results of the numerical simulations are outlined.

The simulation was accomplished for a measuring volume of $120 \times 90 \times 40$ (the unit is set to one). The ratio of the edges is the same as of a on-site fringe projection system available for experimentation.

Further parameters for the simulation are the triangulation angle of 30° between camera and projector, 800×600 camera pixels on the camera plane, 20 markers in direction of X, 15 markers in the direction of Y and 10 markers in the direction of Z on the virtual calibrating plane, 1614 of which are detectable with the camera

image and serve as control points. 9 calibrating planes are used for method B. The order of the polynomials is always $N = 5$.

The virtual test sphere has a radius of $R = 10$ and the center is always at the origin of the object coordinate system (center of the measuring volume), i.e. $\mathbf{r}_c = (0,0,0) \in M$. The influence of some parameters on the deviation of measured values from ideal values is calculated and illustrated for methods A–C. Each time the deviation of the center of the sphere, i.e. $\Delta r_c = \|\mathbf{r}_c - \mathbf{r}_{calc}\|$, and the deviation of the radius, i.e. $\Delta R = R - R_{calc}$, is given.

At first, the influence of the order of the polynomial on the deviation is calculated. Note: The absolute value of the deviation ΔR of the sphere using an order one polynomial is always much bigger than two and, therefore, omitted.

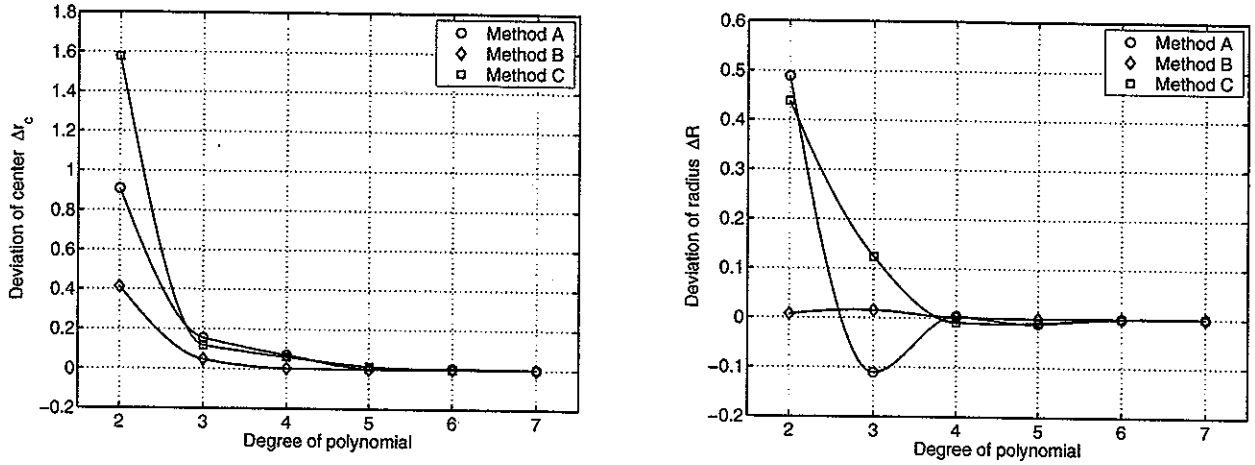

Figure 2. Deviation depending on the order of the polynomial

Method B shows good behavior regarding the deviation of the center of the sphere, that is a result of the accurate determination of the Z-coordinates.

In the second example the number of markers on the calibration plane is altered. The relation between the markers in X, Y and Z direction is 4:3:2, as above. If a number of markers becomes fractional, it is rounded up. Less than 12 markers in X-direction cannot be handled. In this case, there are too few equations for solving the least squares problem.

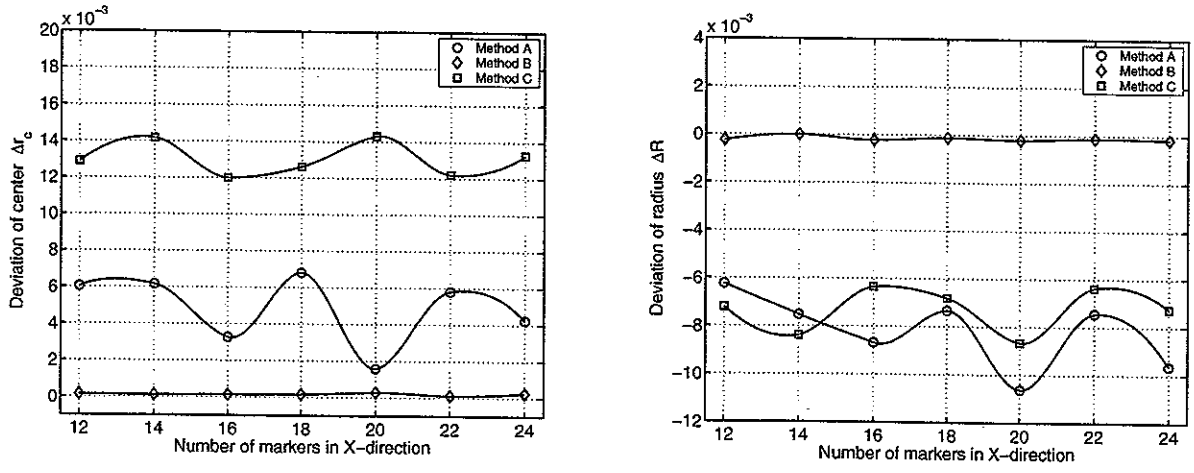

Figure 3. Deviation depending on the number of markers

Fig. 3 shows the result of altering the number of markers. Method B is less influenced by this parameter because the Z-direction is calibrated independent of the number of markers (it uses the whole calibrating plane).

Fig. 4 shows the deviation when the position of center of the test sphere is shifted away from the center of the measuring volume. In this way the behavior of the different calibration methods near the border area of the measuring volume is examined, where possible oscillations may occur. Six different positions are used, starting at the center of the coordinate system and then moving to following positions:

$$\mathrm{r}_c(p) = (50, 35, 10)^{\mathrm{T}} \frac{p}{5} \in M, \qquad p = 0, \ldots, 5$$

Method C shows a quite linear characteristic in this figure, that again is a result of the accurate calculation of

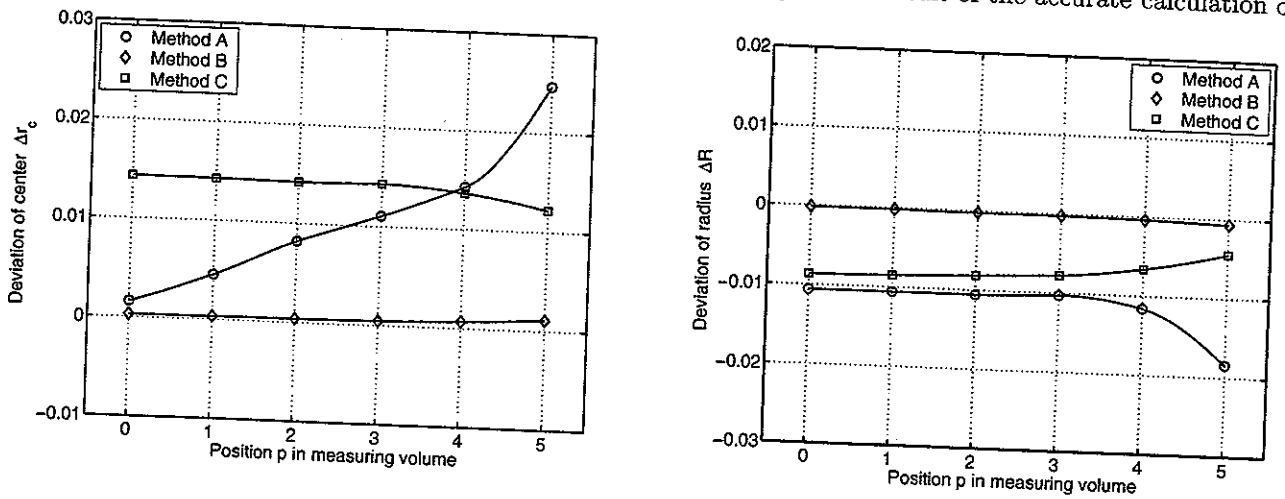

Figure 4. Various positions p of the test sphere in the measuring volume

the Z-coordinates. Concerning the other two methods, A tends to become less accurate when going in direction of the boundary of the measuring volume.

Regarding the numerical calculations itself in general, method B needs tremendous memory space as a result of storing and calculating the coefficients of 800×600 polynomials during the calibration procedure. Because of having to solve many non-linear systems of equations method C is comparatively slow during the calibration of measurement values, whereas method A is comparatively fast, altogether.

4. CONCLUSION

With the virtual fringe projection system it is possible to receive statements about the influence of various measuring parameters on the attainable deviation. Because of the opportunity to individually chose the parameters every influence can be analysed. In particular, various new calibration methods can be evaluated easily. Furthermore, the simulation provides statements about the influence of system parameters which in reality are not or only very hard to achieve, e.g. the optimal number of markers on the calibrating plane or their configuration.

Besides the optimization of the virtual fringe projection system local approximation functions (splines)[6] will be implemented as calibration methods in future as well as a neural network.[7] An extended virtual fringe projection system, e.g. with monte carlo techniques, can be used to estimate the measuring uncertainty of a real fringe projection system.

ACKNOWLEDGMENTS

The author gratefully acknowledge the support of the DFG.

REFERENCES

1. V. Kirschner, W. Schreiber, R. Kowarschik, G. Notni, "Self-calibrating shape system based on fringe projection," in *Rapid Prototyping and Flexible Manufacturing, Proc. SPIE* **3102**, pp. 5–13, 1997.
2. J. Batlle, E. Mouaddib, J. Salvi, "Recent progress in coded structured light as a technique to solve the correspondence problem: a survey," in *Pattern Recognition* **31**(7), pp. 963–982, 1998
3. P. Lehle, H. Gärtner, H.J. Tiziani, C. Voland, "Coded light setups with optimised transformations of code indices," in *Proceedings of SPIE* **2784**, pp. 12–20, 1996.
4. R. Sitnik, M. Kujawinska, J. Woznicki, "Digital fringe projection system for large-volume 360-deg shape measurement", in *Optical Eng.* 41(2), pp. 443–449, 2002.
5. K. Andresen, B. Kamp, R. Ritter, "Three-dimensional surface deformation measurement by a grating method applied to crack tips," in *Optical Eng.* **31**(7), pp. 1499–1504, 1992.
6. K. D. Gremban, C. E. Thorne, T. Kanade, "Geometric camera calibration using systems of linear equations," in *IEEE Trans. on Robotics and Automation* **1**, pp. 562–567, 1988.
7. G. Zhang,Z. Wei, "A novel calibration approach to structured light 3-D vision inspection," in *Optics & Lasers Technology* **34**(5), pp. 373–380, 2002.